Observation of an extremely large nonlinear response in crystalline quartz in THz regime

Zibod, Soheil, Rasekh, Payman, Yildirim, Murat, Bhardwaj, Ravi, Ménard, Jean-Michel, et al.

Soheil Zibod, Payman Rasekh, Murat Yildirim, Ravi Bhardwaj, Jean-Michel Ménard, Robert W. Boyd, Ksenia Dolgaleva, "Observation of an extremely large nonlinear response in crystalline quartz in THz regime," Proc. SPIE 11985, Nonlinear Frequency Generation and Conversion: Materials and Devices XXI, 119850A (4 March 2022); doi: 10.1117/12.2610312

SPIE.

Event: SPIE LASE, 2022, San Francisco, California, United States

Observation of an extremely large nonlinear response in crystalline quartz in THz regime

Soheil Zibod[a], Payman Rasekh[a], Murat Yildrim[b], Ravi Bhardwaj[b], Jean-Michel Ménard[b], Robert W. Boyd[a,b,c], and Ksenia Dolgaleva[a,b]

[a]School of Electrical Engineering and Computer Science, University of Ottawa, Ottawa, Canada
[b]Department of Physics, University of Ottawa, Ottawa, Canada
[c] Institute of Optics, University of Rochester, Rochester, New York, United States

ABSTRACT

We report on the experimental demonstration of nonlinear spectroscopy of crystalline quartz in the terahertz regime. Using accumulated time shift method in the time domain, we observe that with increasing the THz pulse intensity, the experienced delay increases. At higher field intensities, the delay increases with a smaller rate, demonstrating a phase saturation. Analysing the frequency response, we estimate a nonlinear refractive index of the order of 10^{-13} m^2/W which exceeds its value in the visible range by seven orders of magnitude. Furthermore, a negative fifth-order susceptibility of the order of 10^{-30} m^4/V^4 is obtained.

Keywords: THz radiation, Nonlinear refractive index, Crystals

1. INTRODUCTION

Terahertz (THz) radiation, defined as a region in electromagnetic spectrum between microwaves and the far infrared, is gaining a growing importance in applications such as biomedical sensing [1,2], security [3], spectroscopy and imaging[4], and communication[5]. Furthermore, THz time domain spectroscopy (THz-TDs) systems are used for monitoring production processes[6], art conservation [7] and characterizing materials [8].

In addition to the amplitude of the signal, the phase of the signal can be detected by THz-TDs, thus, both real and imaginary parts of refractive index can be retrieved. The development of techniques to generate intense THz radiations extended the research beyond the linear spectroscopy of materials in THz region and made the study of nonlinear behavior of different materials possible; nonlinear effects such as THz induced impact ionisation and inter-valley scattering in semiconductors [9–13], THz high-harmonic generation by hot carriers, [14–16] and THz induced ferroelectricity and collective coherence control[17,18]

Extreme THz-induced Kerr effects have been reported and predicted for water vapor[19], different liquids [20–22] and solids[23–25], where the nonlinear refractive indices can be several orders of magnitude larger than their values in the optical regime.

In this Article, we report on the nonlinear behavior of crystalline quartz in terahertz regime. First, we perform nonlinear THz-TDS on crystalline quartz sample. Then, we performed the accumulated time shift analysis. The results show how the increase in the pulse intensity of the THz radiation changes the delay experienced by the pulse. Next, the analysis in the Fourier domain reveals an increase in the nonlinear phase and nonlinear absorption with the increase of field intensity. At higher signal levels, the nonlinear phase growth with respect to field intensity slows down, whereas the nonlinear absorption grows further. Furthermore, extremely large values for the nonlinear refractive index and fifth order susceptibility are obtained, where the latter has a negative real part.

Further author information: (Send correspondence to Soheil Zibod)
Soheil Zibod: E-mail: szibo043@uottawa.ca

Nonlinear Frequency Generation and Conversion: Materials and Devices XXI, edited by Peter G. Schunemann, Valentin Petrov, Proc. of SPIE Vol. 11985, 119850A
 · 0277-786X · doi: 10.1117/12.2610312

2. EXPERIMENTAL DETAILS

The intense THz radiation is generated in an optical rectification process in lithium niobate, where the pulse-front tilting technique is used to make the process phase-matched and efficient[26]. The setup schematic is depicted in Figure 1 . The beam, coming from a 800 nm Ti:sapphire laser with a pulse duration of 45 fs and repetition rate of 1kHz, is split into pump and probe paths. In the pump path, the beam diffracts from a grating and after passing through two cylindrical lenses, it propagates in the generation crystal. The generated THz radiation is collimated and focused with a number of gold off-axis parabolic mirrors. A pair of wire-grid polarizers is used to control the THz field amplitude during the measurements.

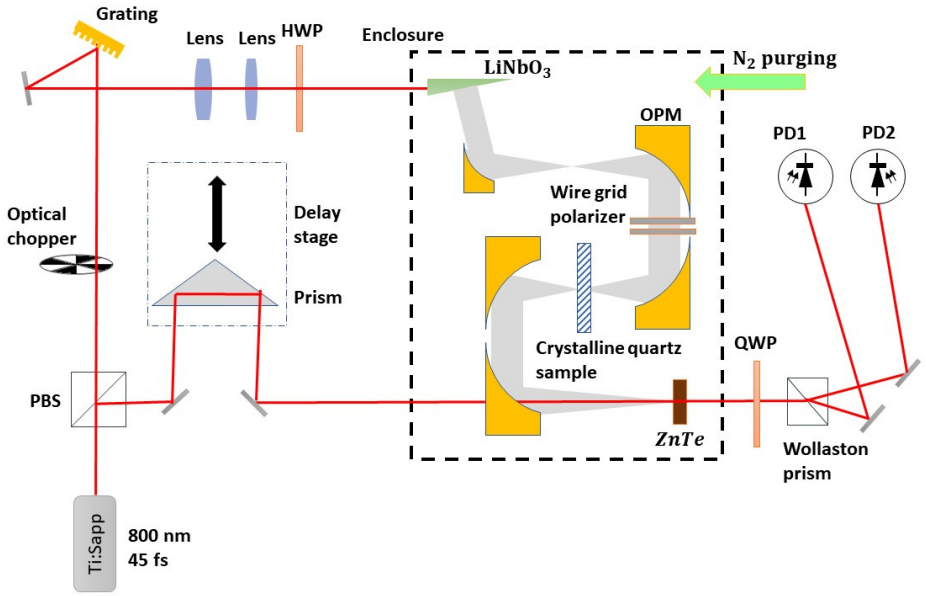

Figure 1: THz-TDS experimental setup. Off-axis parabolic mirror (OPM)s are used to focus and collimate THz beam. Half wave plate (HWP), quarter wave plates (QWP) and polarizing beam splitters (PBS) are used in the setup.

In the probe path, the probe beam and THz beam copropagate inside the 200 μm thick ZnTe detection crystal. A delay stage is also used to change the overlap time between THz and probe beam, so that different points of the signal are measured. As the THz pulse propagates through the detection crystal, the refractive index experienced by the probe beam is modified through linear electro-optic effect, resulting in the birefringence in the crystal. The phase difference induced by the birefringence is then converted into the beam ellipticity using a quarter-wave plate. Finally, the beam ellipticity is translated into the differential electric signal using a Wollastron prism followed by a balanced photodetector pair connected to the lock-in amplifier. The peak amplitude of the electric field is estimated to be 225 kV/cm at the focal position, at where a 1mm thick crystalline quartz sample is placed. To eliminate the water vapor absorption, the part of the setup where THz beam propagates, is enclosed, and purged with nitrogen. Different field amplitudes are obtained by rotating the first wire-grid polarizer and keeping the second fixed.

3. RESULTS AND DISCUSSION

The time domain signals for different signal levels for both free space and crystalline quartz sample are shown in Figure 2. We observe that with increasing the field amplitude, the pulse experiences further delay with respect to the lowest signal level of 25 kV/cm. A linear refractive index of 2.11 is also obtained which is in a good agreement with the literature[27].

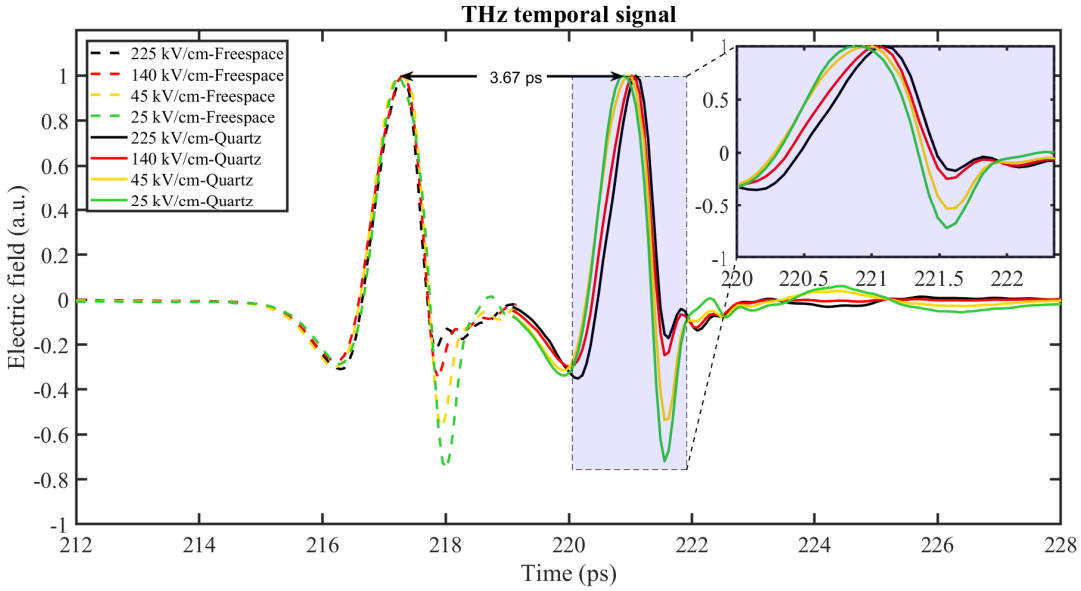

Figure 2: THz time domain signal in freespace (dashed) and crystalline quartz (solid) for different signal levels. The inset shows the increasing delay experienced in quartz.

Figure 3 shows the accumulated time shift for each of the signal levels compared to the lowest level, where the time shift for each level is calculated by

$$t(s_i) = \frac{1}{N}\sum_{k}^{N} t(V_i = V_k) - t(V_{low} = V_k) \tag{1}$$

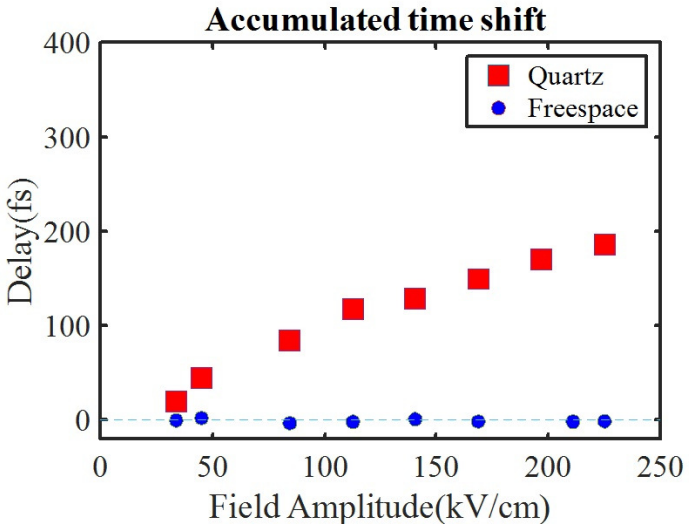

Figure 3: The accumulated time shift in free space (blue) and crystalline quartz (red) for different signal levels.

where $t(s_i)$ is the averaged time shift, V_i is the ith signal and V_{low} is the lowest level signal. The analysis is performed over the main lobe as it represents most of the THz features. The delay experienced by the pulse increases with the increase of the field amplitude. However, as the field amplitude grows further, the nonlinear delay grows at a lower pace, suggesting a saturation effect in the nonlinear phase.

Figure 4 shows the spectral density for the quartz sample and free space in the frequency range between 0.3 to 2 THz. We observe as the signal level increases, the difference between the free space spectrum and quartz sample increases, revealing an increase in the absorption.

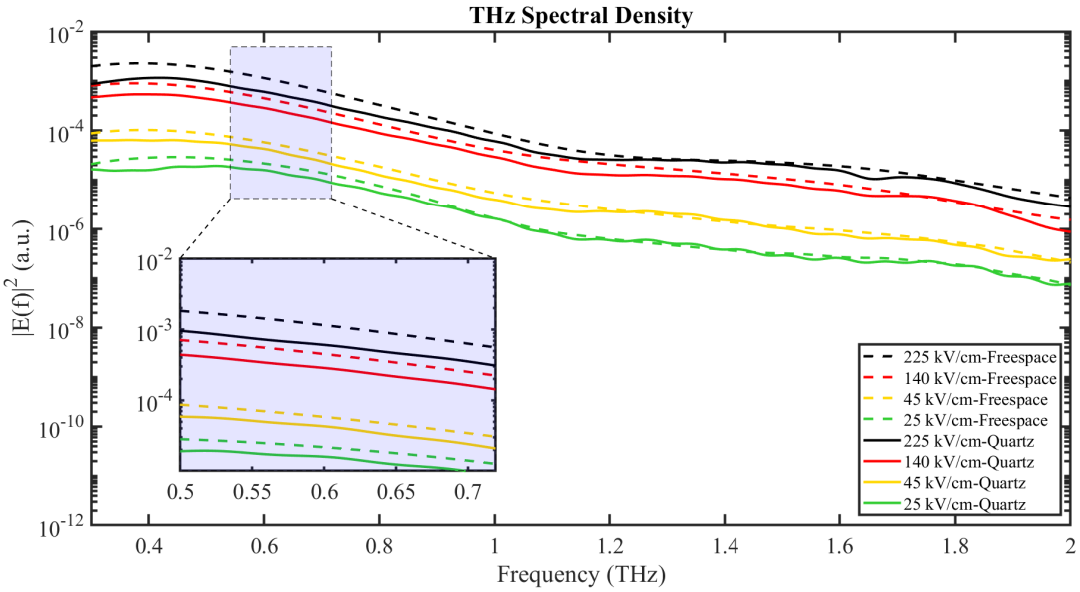

Figure 4: Signal spectral density for free space (dashed) and quartz (solid). The difference between free space signal and quartz signal increases as the signal level increases.

Figure 5a shows the nonlinear phase experienced by the signal for different intensity levels at 0.5 THz, where the spectral density is maximum.It indicates that as intensity increases, the nonlinear phase cannot be expressed with a single linear term and suggests a negative higher order nonlinearity term. The differential nonlinear phase for the higher signal is related to the intensity by

$$\begin{aligned}\phi_i^{NL}(\omega) &= \phi_i(\omega) - \phi_{low}(\omega) \\ &= n_2(\omega) I_i \frac{\omega}{c} d + n_4(\omega) I_i^2 \frac{\omega}{c} d \end{aligned} \tag{2}$$

where ϕ_i is the total phase of the i-th signal and ϕ_{low} is the phase experienced by the lowest signal, as the linear response of the material.n_2 and n_4 are second-order and fourth-order nonlinear refractive indices, respectively. Finally, I_i is the peak intensity of the i-th level signal.

The absorption coefficient of crystalline quartz is depicted in Figure 5b. The absorption coefficient of the material can be expressed as

$$\alpha_i(\omega) = \alpha_0(\omega) + \beta_2(\omega) I_i + \beta_4(\omega) I_i^2 \tag{3}$$

where α_i ,α_0 , β_2 and β_4 are total absorption coefficient for i-th signal, linear absorption coefficient, second-order nonlinear absorption coefficient and fourth-order absorption coefficient, respectively.

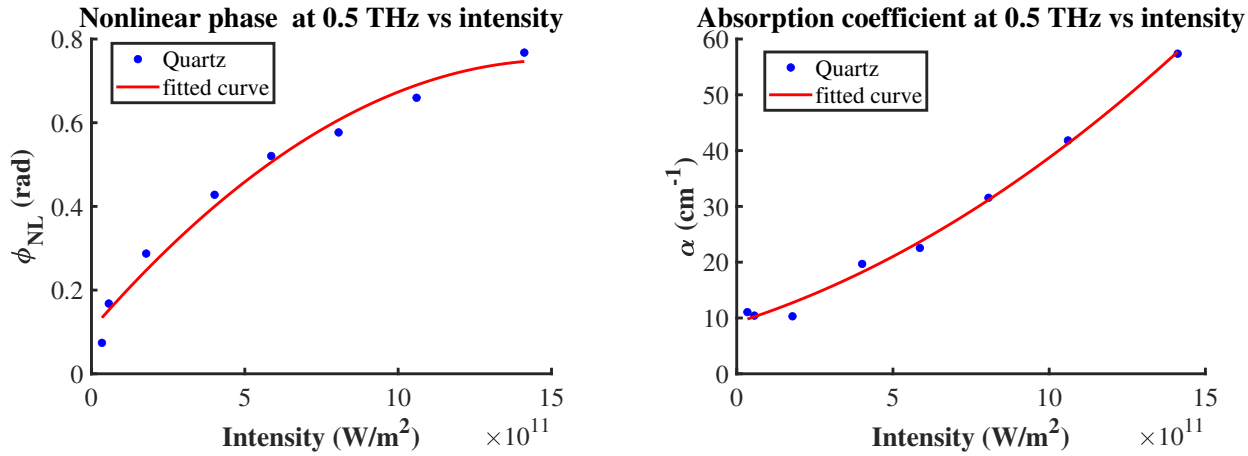

(a) (b)

Figure 5: (a) nonlinear phase for different intensities at 0.5THz (b) absorption coefficient for different intensities at 0.5THz

The measurements show $n_2 = 8 \times 10^{-14}$ m^2/W, $n_4 = -2.6 \times 10^{-26}$ m^4/W^2, $\beta_2 = 1.1 \times 10^{-10}$ m/W and $\beta_4 = 5 \times 10^{-23}$ m^3/W^2. The complex third-order and fifth-order nonlinear susceptibility are found as $\chi^3 = (1.3 \times 10^{-15} + i8.4 \times 10^{-17})$ m^2/V^2 and $\chi^5 = (-2.7 \times 10^{-30} + i2.5 \times 10^{-31})$ m^4/V^4, respectively. In the lower intensities, the dominant effect is χ^3 making the relation nonlinear phase and absorption coefficient linearly proportional to the pulse intensity. However, as the intensity surpasses 600 GW/m^2, the χ^5 also reveals itself, being responsible for the decrease and increase in the nonlinear phase and absorption coefficient growth rates, respectively. The calculated value of the n_2 is approximately seven orders of magnitude larger than the value for the fused silica at optical frequencies.

4. CONCLUSION

We observed an extremely large nonlinear response of crystalline quart in the THz region. Time domain spectroscopy was carried out on a crystalline quartz sample. The accumulated time shift analysis showed that in addition to the χ^3 effect on the nonlinear phase, we also have a negative χ^5 that suppress the nonlinear phase at higher intensities. Using the Fourier analysis, we calculated an $n_2 = 8 \times 10^{-14}$ m^2/W, which is several orders of magnitude larger than its value for silica in optical regime.

ACKNOWLEDGMENTS

This work was supported by the Canada Excellence Research Chairs program, Canada Research Chairs program and the National Science and Engineering Research Council of Canada (NSERC) Discovery and Strategic programs.

REFERENCES

[1] Peng, Y., Shi, C., Wu, X., Zhu, Y., and Zhuang, S., "Terahertz imaging and spectroscopy in cancer diagnostics: A technical review," *BME Frontiers* **2020**, 2547609 (Sep 2020).

[2] Lindley-Hatcher, H., Stantchev, R. I., Chen, X., Hernandez-Serrano, A. I., Hardwicke, J., and Pickwell-MacPherson, E., "Real time thz imaging—opportunities and challenges for skin cancer detection," *Applied Physics Letters* **118**(23), 230501 (2021).

[3] Chen, J., Chen, Y., Zhao, H., Bastiaans, G. J., and Zhang, X.-C., "Absorption coefficients of selected explosives and related compounds in the range of 0.1–2.8 thz," *Opt. Express* **15**, 12060–12067 (Sep 2007).

[4] Jepsen, P., Cooke, D., and Koch, M., "Terahertz spectroscopy and imaging – modern techniques and applications," *Laser & Photonics Reviews* **5**(1), 124–166 (2011).

[5] Kleine-Ostmann, T. and Nagatsuma, T., "A review on terahertz communications research," *Journal of Infrared, Millimeter, and Terahertz Waves* **32**, 143–171 (Feb 2011).

[6] Krumbholz, N., Hochrein, T., Vieweg, N., Hasek, T., Kretschmer, K., Bastian, M., Mikulics, M., and Koch, M., "Monitoring polymeric compounding processes inline with thz time-domain spectroscopy," *Polymer Testing* **28**(1), 30–35 (2009).

[7] Krügener, K., Schwerdtfeger, M., Busch, S. F., Soltani, A., Castro-Camus, E., Koch, M., and Viöl, W., "Terahertz meets sculptural and architectural art: Evaluation and conservation of stone objects with t-ray technology," *Scientific Reports* **5**, 14842 (Oct 2015).

[8] Busch, S., Weidenbach, M., Fey, M., Schäfer, F., Probst, T., and Koch, M., "Optical properties of 3d printable plastics in the thz regime and their application for 3d printed thz optics," *Journal of Infrared, Millimeter, and Terahertz Waves* **35**(12), 993–997 (2014).

[9] Ašmontas, S., Bumelienė, S., Gradauskas, J., Raguotis, R., and Sužiedėlis, A., "Impact ionization and intervalley electron scattering in insb and inas induced by a single terahertz pulse," *Scientific Reports* **10**, 10580 (Jun 2020).

[10] Hoffmann, M. C., Hebling, J., Hwang, H. Y., Yeh, K.-L., and Nelson, K. A., "Impact ionization in insb probed by terahertz pump—terahertz probe spectroscopy," *Phys. Rev. B* **79**, 161201 (Apr 2009).

[11] Lange, C., Maag, T., Hohenleutner, M., Baierl, S., Schubert, O., Edwards, E. R. J., Bougeard, D., Woltersdorf, G., and Huber, R., "Extremely nonperturbative nonlinearities in gaas driven by atomically strong terahertz fields in gold metamaterials," *Phys. Rev. Lett.* **113**, 227401 (Nov 2014).

[12] Tarekegne, A. T., Iwaszczuk, K., Zalkovskij, M., Strikwerda, A. C., and Jepsen, P. U., "Impact ionization in high resistivity silicon induced by an intense terahertz field enhanced by an antenna array," **17**, 043002 (apr 2015).

[13] Tani, S., Blanchard, F. m. c., and Tanaka, K., "Ultrafast carrier dynamics in graphene under a high electric field," *Phys. Rev. Lett.* **109**, 166603 (Oct 2012).

[14] Schubert, O., Hohenleutner, M., Langer, F., Urbanek, B., Lange, C., Huttner, U., Golde, D., Meier, T., Kira, M., Koch, S. W., and Huber, R., "Sub-cycle control of terahertz high-harmonic generation by dynamical bloch oscillations," *Nature Photonics* **8**, 119–123 (Feb 2014).

[15] Hafez, H. A., Kovalev, S., Deinert, J.-C., Mics, Z., Green, B., Awari, N., Chen, M., Germanskiy, S., Lehnert, U., Teichert, J., Wang, Z., Tielrooij, K.-J., Liu, Z., Chen, Z., Narita, A., Müllen, K., Bonn, M., Gensch, M., and Turchinovich, D., "Extremely efficient terahertz high-harmonic generation in graphene by hot dirac fermions," *Nature* **561**, 507–511 (Sep 2018).

[16] Chai, X., Ropagnol, X., Raeis-Zadeh, S. M., Reid, M., Safavi-Naeini, S., and Ozaki, T., "Subcycle terahertz nonlinear optics," *Phys. Rev. Lett.* **121**, 143901 (Oct 2018).

[17] Qi, T., Shin, Y.-H., Yeh, K.-L., Nelson, K. A., and Rappe, A. M., "Collective coherent control: Synchronization of polarization in ferroelectric pbtio$_3$ by shaped thz fields," *Phys. Rev. Lett.* **102**, 247603 (Jun 2009).

[18] Li, X., Qiu, T., Zhang, J., Baldini, E., Lu, J., Rappe, A. M., and Nelson, K. A., "Terahertz field–induced ferroelectricity in quantum paraelectric srtio¡sub¿3¡/sub¿," *Science* **364**(6445), 1079–1082 (2019).

[19] Rasekh, P., Safari, A., Yildirim, M., Bhardwaj, R., Ménard, J.-M., Dolgaleva, K., and Boyd, R. W., "Terahertz nonlinear spectroscopy of water vapor," *ACS Photonics* **8**(6), 1683–1688 (2021).

[20] Tcypkin, A., Zhukova, M., Melnik, M., Vorontsova, I., Kulya, M., Putilin, S., Kozlov, S., Choudhary, S., and Boyd, R. W., "Giant third-order nonlinear response of liquids at terahertz frequencies," *Phys. Rev. Applied* **15**, 054009 (May 2021).

[21] Hoffmann, M. C., Brandt, N. C., Hwang, H. Y., Yeh, K.-L., and Nelson, K. A., "Terahertz kerr effect," *Applied Physics Letters* **95**(23), 231105 (2009).

[22] Tcypkin, A. N., Melnik, M. V., Zhukova, M. O., Vorontsova, I. O., Putilin, S. E., Kozlov, S. A., and Zhang, X.-C., "High kerr nonlinearity of water in thz spectral range," *Opt. Express* **27**, 10419–10425 (Apr 2019).

[23] Dolgaleva, K., Materikina, D. V., Boyd, R. W., and Kozlov, S. A., "Prediction of an extremely large nonlinear refractive index for crystals at terahertz frequencies," *Phys. Rev. A* **92**, 023809 (Aug 2015).

[24] Zalkovskij, M., Strikwerda, A. C., Iwaszczuk, K., Popescu, A., Savastru, D., Malureanu, R., Lavrinenko, A. V., and Jepsen, P. U., "Terahertz-induced kerr effect in amorphous chalcogenide glasses," *Applied Physics Letters* **103**(22), 221102 (2013).

[25] Francis, K. J. G., Chong, M. L. P., E, Y., and Zhang, X.-C., "Terahertz nonlinear index extraction via full-phase analysis," *Opt. Lett.* **45**, 5628–5631 (Oct 2020).

[26] Hebling, J., Yeh, K.-L., Hoffmann, M. C., Bartal, B., and Nelson, K. A., "Generation of high-power terahertz pulses by tilted-pulse-front excitation and their application possibilities," *J. Opt. Soc. Am. B* **25**, B6–B19 (Jul 2008).

[27] Davies, C. L., Patel, J. B., Xia, C. Q., Herz, L. M., and Johnston, M. B., "Temperature-dependent refractive index of quartz at terahertz frequencies," *Journal of Infrared, Millimeter, and Terahertz Waves* **39**, 1236–1248 (Dec 2018).